novel analytical approaches to characterize particles in biopharmaceuticals
Grabarek, A.D.

Citation
Grabarek, A. D. (2021, October 21). *novel analytical approaches to characterize particles in biopharmaceuticals*. Retrieved from https://hdl.handle.net/1887/3217865

Chapter 2

Critical evaluation of microfluidic resistive pulse sensing for quantification and sizing of nanometer- and micrometer-sized particles in biopharmaceutical products

Adam D. Grabarek[1,2], Daniel Weinbuch[1], Wim Jiskoot[1,2]*, Andrea Hawe[1]*

[1]*Coriolis Pharma, Fraunhoferstrasse 18 b, 82152 Martinsried, Germany*

[2]*Leiden Academic Centre for Drug Research, Leiden University, The Netherlands*

corresponding authors

Abstract

The objective was to evaluate performance, strengths and limitations of the microfluidic resistive pulse sensing (MRPS) technique for the characterization of particles in the size range from about 50 to 2000 nm. MRPS, resonant mass measurement (RMM), nanoparticle tracking analysis (NTA) and dynamic light scattering (DLS) were compared for the analysis of nanometer-sized polystyrene (PS) beads, liposomes, bacteria and protein aggregates. An electrical conductivity of at least 3 mS/cm (equivalent to 25 mM NaCl) was determined as a key requirement for reliable analysis with MRPS. Particle size distributions of PS beads determined by MRPS, NTA and RMM correlated well. However, counting precision varied significantly among the techniques, and was best for RMM followed by MRPS and NTA. As determined by measuring single and mixed PS bead populations, MRPS showed the highest peak resolution for sizing. RMM and MRPS were superior over DLS and NTA for the characterization of stressed protein samples. Finally, MRPS proved to be the only analytical technique able to characterize both bacteria and liposomes. In conclusion, MRPS is an orthogonal technique alongside other established techniques for a comprehensive analysis of a sample´s particle size distribution and particle concentration.

Introduction

Particles ranging from a few nanometers up to several hundred micrometers receive substantial attention in the biopharmaceutical industry, for example, as unwanted particulate impurities in drug products, as drug delivery systems (e.g., liposomes) and as active pharmaceutical ingredients (APIs, e.g., virus-like particles, viruses, exosomes, bacteria, cells)[1,2].

Particulate impurities found in therapeutic protein drug products can have various sources and may include environmental contaminants, impurities related to excipients or degradants of excipients, and proteinaceous particles formed due to instability of the API[3]. Particulate impurities can impair product stability, quality and safety, and may cause serious adverse effects in patients, such as capillary occlusion, hypersensitivity reactions and neutralizing antibody formation[4-6]. The wide size range and heterogeneous distribution of protein aggregates and other impurities pose a great challenge in protein drug development and quality control. Since no current analytical technique is able to comprehensively characterize the entire protein aggregate population, several complementary methods must be utilized[7-9]. Even though regulatory authorities increasingly demand the characterization of protein therapeutics within the nanometer size range[10], technical limitations of currently available instruments with respect to robustness and low throughput make the development and validation of methods to size and quantify particles within this range extremely challenging[11,12].

Drug delivery systems within the nanometer size range (e.g., liposomes, polymer-based nanoparticles) are often applied to control the biodistribution profile of small and large molecules, to promote their selective and specific targeted release, or to protect the API from proteolytic degradation upon administration[1,13]. The efficacy and safety of nanoparticulate formulations depend to a significant extent on their size, quantity and heterogeneity[14]. In addition, utilization of genetically engineered microbes and viruses has become a promising tool for therapies against life-threatening diseases, such as cancer[15]. For all of these therapeutic agents, adequate particle characterization methods are required for the determination of product quality.

Currently, common techniques used for particle characterization in the nanometer and low micrometer size ranges include transmission electron microscopy[9,16], flow cytometry[12], dynamic light scattering (DLS)[17,18], asymmetrical flow field-flow fractionation[19], resonant mass measurement (RMM)[18,20,21] and nanoparticle tracking analysis (NTA)[22-25]. Each of these techniques has its own strengths and limitations, based on a distinct measurement principle, and covers a specific size range[9,23,26]. Despite the availability of several methods, our ability to characterize particle populations within the nanometer and low micrometer size ranges is limited and analytical gaps remain[27].

Resistive pulse sensing has been widely reported as a technique for characterization of single molecules as well as particles sizing up to several micrometers[28]. It is based on the electrical sensing zone technique, or Coulter principle, where the size of a particle is measured based on the resistance change it induces upon passage through a small orifice. The technique was primarily developed for counting and sizing of human cells. With the advancement of microfluidics, microfluidic resistive pulse sensing (MRPS) based methods have been developed. The MRPS technology is employed in nCS1, which utilizes disposable polydimethylsiloxane (PDMS) cartridges for particle sizing and counting. The covered size range is cartridge dependent and ranges from about 50 to 2000 nm. In order to characterize particles within this range, four types of cartridges are available, namely TS-300 (50-300 nm), TS-400 (65-400 nm), TS-900 (130-900 nm) and TS-2000 (250- 2000 nm). The principal component of the cartridge is the sensing electrode, which is fixed between a fluidic resistor and a nanoconstriction. The motion of the analyte with suspended particles is controlled within the microfluidic channels with pressurized air. Particles are directed through the orifice of the nanoconstriction where a single passage induces a change in the electric current. This event is characterized by an induced nanoconstriction resistance (ΔR) which changes the fluid potential (ΔV) in contact with the sensing electrode. Its magnitude then depends, accordingly to the Maxwell's equation[29], on the occupied volume by the particle at the constriction, and thus particle size, as described in more detail elsewhere[30].

Recently, Barnett et al. performed a comparison of nCS1 to light scattering-based techniques, such as DLS and size exclusion chromatography with multi-angle static light

scattering, for the characterization of silicone oil droplets and protein particles in formulations exposed to various stress conditions[31]. In our study, we extended the investigation of MRPS by exploring the potential and limitations of nCS1 for the characterization of various types of nanometer-sized particles with special focus on biological applications. In addition, a direct comparison of MRPS with other submicron particle characterization techniques, i.e., DLS, NTA and RMM, which are commonly applied during biopharmaceutical drug product development, was performed to assess each method's strengths and weaknesses.

Materials and Methods

Materials

Polysorbate 20, sodium chloride and ten-fold concentrated phosphate buffer saline (PBS) were obtained from Sigma-Aldrich (Steinheim, Germany). Dibasic and monobasic sodium phosphate was purchased from VWR (Bruchsal, Germany). In-house Milli-Q water (resistivity 18.2 MΩ cm) was dispensed from an Advantage A10 purification system (Millipore, Newark, New Jersey). All diluents used in the study were freshly filtered using a 0.1 µm Millex-VV syringe filter unit (Millipore, Schwalback, Germany) and dilutions were performed under laminar air flow conditions.

Polystyrene (PS) nanometer standard beads with diameters of 203 ± 5 nm (PS203nm), 297 ± 7 nm (PS297nm), 495 ± 8 nm (PS495nm), 799 ± 9 nm (PS799nm) and 1030 ± 9 nm (PS1030nm) were purchased from Fisher Scientific (Ulm, Germany). Dilutions of the PS beads were performed in formulation buffer containing 0.1% w/v polysorbate 20, unless otherwise stated.

Preparation of proteinaceous particles

Bovine serum albumin (BSA) (Sigma-Aldrich, Steinheim, Germany; LOT 193829) was used to generate proteinaceous particles. A 10 mg/mL protein solution was prepared by dissolving lyophilized BSA in single strength PBS (pH adjusted to 4.75 with 1 M HCl). The solution was filtered by using a 0.1-µm polyethersulfone syringe filter and 1-mL aliquots were artificially stressed in 2-mL Eppendorf tubes by using a Thermomixer (Eppendorf, Hamburg, Germany) at 67 °C/1400 rpm for 5 min. In order to homogenize the sample, aliquots were pooled into a Falcon tube and subsequently aliquoted into 1.5-mL Eppendorf tubes for long term storage at -80 °C. Thawed aliquots were measured with Micro-Flow Imaging and DLS to demonstrate vial-to-vial consistency (n=3) as well particle stability at room temperature over 8 hours (data not shown). To obtain optimal proteinaceous particle concentrations for each analytical technique, the thawed samples were diluted with PBS (pH 7.4).

Preparation of liposomes

Negatively charged liposomes (-21 mV, determined with Zetasiser nano ZS), composed of distearoyl phophatidylcholine, distearoyl phosphatidylglycerol and cholesterol, were kindly provided by Naomi Benne (Leiden Academic Centre for Drug Research) and were prepared as described elsewhere[32].

Preparation of probiotic bacterial samples

Pharmaceutical-grade probiotic bacteria containing two strains of Lactobacillus (*L. helveticus* R-52 and *L. rhamnosus* R-11) were purchased as Lacidofil from Institut Rosell Inc., Montreal, CA. About 40 mg of the capsule's dry powder blend was dissolved in 10 mL of 150 mM NaCl in a 15-mL Falcon tube (VWR, Bruchsal, Germany) and mixed at 10 rpm for 15 min by using a rotating mixer. Volume-based dilutions in 150 mM NaCl were performed and samples were measured within 2 hours post preparation.

Dynamic light scattering (DLS)

DLS was performed by using a Zetasizer Nano ZS (Malvern Instruments, Worcestershire, UK) equipped with a 633-nm He-Ne laser set at an angle of 173°. Single-use PS semi-micro

cuvettes with a 10-mm path length (Brand, Wertheim, Germany) were filled with 0.5 ml of sample for each measurement. The attenuator was set automatically depending on the particle concentration. Samples were equilibrated to a working temperature of 25 °C for 60 seconds prior to each analysis. The Z-average diameter (Z-ave), polydispersity index (PDI) and intensity-weighted size distribution were derived from the autocorrelation function by using the Dispersion Technology Software version 6.01 with CONTIN smoothing algorithm. Each measurement was performed in triplicate.

Nanoparticle tracking analysis (NTA)

NTA data was obtained with a NanoSight (Model LM20, Malvern Instrument, Malvern, UK) instrument with a 405-nm laser (blue), a sample chamber and a Viton fluoroelastomer O-ring. Samples were injected into the chamber by using a 1-mL silicone-free syringe and the purging volume was 0.3 mL. A video capture was initiated immediately after injection and a triplicate measurement of 60-second replicates was performed. All measurements were collected at room temperature with camera levels set to optimal values and 200 valid tracks must have been recorded for a valid measurements. Data collection and evaluation was done with the NanoSight software version 3.2, unless otherwise stated.

Resonant mass measurement (RMM)

Particles were analyzed with a Archimedes system (Malvern Instrument, Malvern, UK) equipped with a Hi-Q Micro Sensor (Malvern Instrument) operated by a ParticleLab software version 2.01. Prior to each set of measurements, the instrument was calibrated with PS1030nm followed by a measurement of Milli-Q water to confirm cleanliness of the system. Between sample measurements two "sneeze" operations were performed and the system was flushed for 5 minutes with Milli-Q water to avoid carry-over. Samples were loaded for 40 seconds and the limit of detection (LOD) was determined automatically by the software. A density value of 1.05 g/cm^3 was used for PS beads, 1.34 g/cm^3 for protein particles and 1.16 g/cm^3 for bacteria[33], and solely negatively buoyant particles were considered. Measurements were performed in triplicate and for each replicate 150 nL was analyzed, where a minimum of 50 particle counts were recorded.

Microfluidic resistive pulse sensing (MRPS)

Microfluidics-based resistive pulse sensing measurements were performed by using an nCS1 instrument (Spectradyne, Torrence, USA) equipped with disposable PDMS cartridges: TS-400 (size range 65-400 nm), TS-900 (size range 125-900 nm) and TS-2000 (size range 250-2000 nm). A running buffer of PBS (pH 7.4) with 1% w/v polysorbate 20 was used to generate an appropriate ionic electrical current in the analyte and ensure an appropriate flow of particles leaving the cartridge to the waste reservoirs. The running buffer does not have contact with the analyte prior to the nano-constriction, thereby avoiding cross-contamination. Approximately 3 µL of sample was used for each measurement and not less than 500 particles were counted per analysis. To achieve appropriate sizing of the analyzed particles, a calibration step for each cartridge was required. Calibration was performed by using PS beads (495 ± 8 nm) diluted in analyte's diluent consisting of 0.1% polysorbate 20. Collected data was analyzed by using nCS1 Data Analyzer (Spectradyne, Torrence, USA). Filters were applied for data analysis in order to exclude false-positive signals. The used filters excluded detected particle events characterized by user defined transit time, signal-to-noise ratio, peak symmetry and/or diameter.

Conductivity measurements

Electric conductivities of samples were measured in triplicate at 25 °C by using a SevenCompact S230 basic conductivity meter (Mettler Toledo, Columbus, USA), calibrated with a 1.413 µS/cm standard

Results

Impact of conductivity on sample analysis by MRPS

At first, the impact of conductivity on the MRPS technique's performance for particle sizing and counting was investigated. A consistent precision of measurement of the mean diameter and concentration of PS1030nm beads suspended in solutions with a conductivity ranging from ~3 mS/cm (equivalent to 25 mM NaCl) up to ~17 mS/cm (150 mM NaCl) could be achieved, independent of pH and ionic species (Figure 1). Below ~3 mS/cm, however,

there is a notable decrease in the measured mean diameter as well as an increase in particle count. The higher baseline noise (Figure 2 A, 2 B and Supplementary figure S1) increases the limit of detection. The overestimated particle concentration at low electrical conductivity is related to the measuring principle of MRPS. Media with low ionic strength lead to an increased detected transit time of a particle passing through the nanoconstriction, as shown in Figure 2 C (see also discussion section).
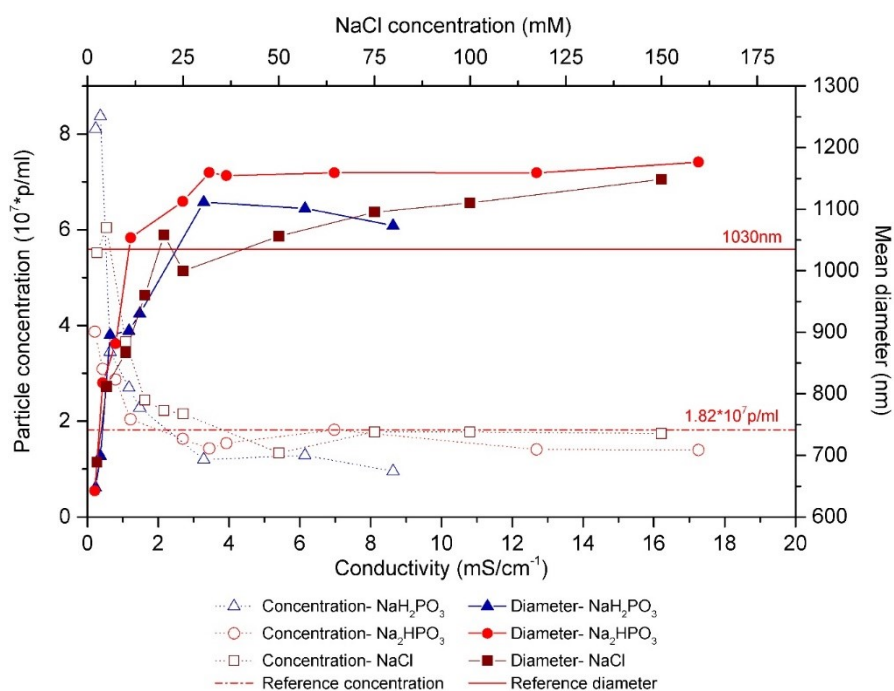

Figure 1: Sizing and quantification of PS1030 beads suspended in solutions with increasing ionic strength using cartridge TS-2000. The top x-axis shows the molar concentration of NaCl corresponding to the electrical conductivity values at the bottom x-axis. Each data point represents a single measurement. Horizontal solid and dashed lines indicate the reference particle size and concentration, respectively, specified by the manufacturer.
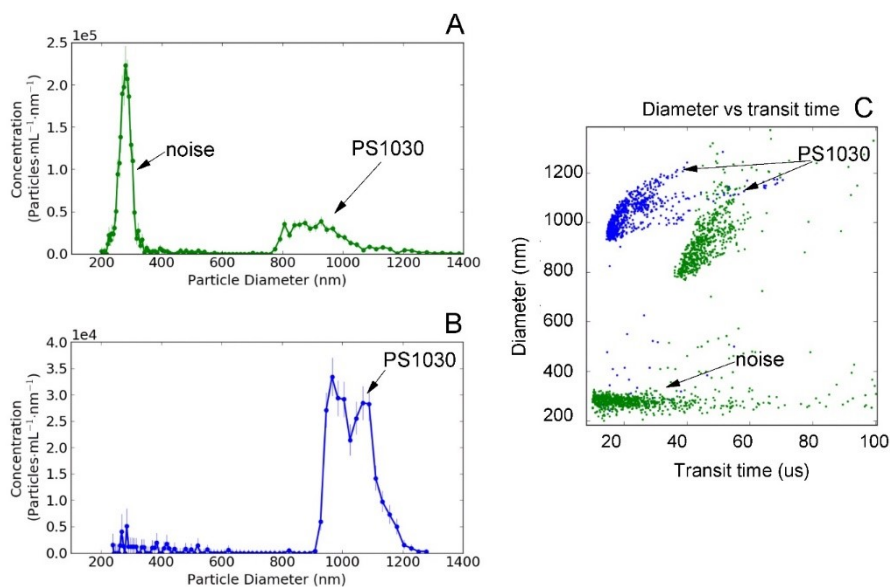
Figure 2: Particle size distribution characterized with MRPS (nCS1 equipped with a TS-2000 cartridge) for PS1030nm beads suspended in Na2HPO4 solution with low Na2HPO4 concentration (5 mM) (a) and high Na2HPO4 concentration (150 mM) (b). Scatter plot of measured diameter versus transit time for PS1030nm at high (blue) and low (green) Na2HPO4 concentration (c).

Repeatability of sizing and counting of monodisperse nanoparticles by MRPS

Repeatability was assessed by comparing the detected particle concentration, mean and mode diameter size in nm, as well as peak centroid of five replicate measurements of PS495nm and PS1030nm suspended in single strength PBS with 0.1% polysorbate 20 (conductivity ~14 mS/cm) by using TS-900 and TS-2000 cartridges, respectively. The results obtained from measurements performed with one single cartridge (intra-cartridge variability) and with multiple cartridges (inter-cartridge variability) from a single batch were used to calculate the CV% of replicate measurements (Table 1). For each of the measured parameters, the variance of the replicate intra- and inter-cartridge measurements was statistically equal (one-sided ANOVA, *p< 0.05 confidence level) for both cartridge types.

Table 1. Comparison of MRPS repeatability in sizing and counting of PS495nm and PS1030nm in five replicate measurements using single (intra) and multiple (inter) cartridges for two types of cartridges (TS-2000 and TS-900). PS beads were suspended in PBS (pH 7.4) with 0.1% w/v polysorbate 20.

Measurement	Cartridge type	Bead size (nm)	Particle concentration (p/ml)	Mean diameter (nm)	Mode diameter (nm)	Centroid (nm)
			Coefficient of variation (%)			
Inter	TS-2000	1030 ± 9	6.45	5.18	7.27	4.71
Intra			7.11	3.42	5.53	6.34
Inter	TS-900	495 ± 8	13.98	5.11	5.14	5.06
Intra			19.42	4.10	4.20	4.48

Accuracy and precision of MRPS compared to DLS, NTA and RMM using monodisperse nanoparticles

Accuracy and precision for sizing and counting of triplicate measurements of monodisperse PS beads were compared for DLS, NTA, RMM and MRPS. Because of the differences in the working size ranges of each technique, two distinct PS bead sizes were selected to perform a cross comparison between all four techniques.

Size accuracy was determined based on comparing the mean size diameter, peak maximum, and particle size distribution defined as span, calculated as $((D_{90}-D_{10})/D_{50})$, and percentile values at 10%, 50% and 90% (D_{10}, D_{50}, D_{90}). Sizing precision of each technique was evaluated based on the standard deviation of the above mentioned values over the replicate measurements. The estimated particle concentration of the PS standard sizing beads was calculated based on the size-, density- and mass-concentration values specified by the manufacturer. This approach was chosen because, to the best of our knowledge, there are no certified counting standard beads available in the required size range.

As the concentration of the PS sizing beads is not traceable, and the concentration is based on an estimation, absolute counting accuracy could not be tested. Therefore, a relative comparison between the techniques in particle counting and examination of the precision in determination of particle concentration was done instead. The stated particle concentration limits for TS-900 and TS-2000 are estimates based on the PS bead specifications from the manufacturer.

For both PS bead populations, a good agreement in the determined mean diameter and maximum peak position was found among all evaluated techniques (Table 2). DLS measurements of both PS bead standards resulted in ca. 10% greater size values compared to the single particle counting techniques. RMM provided lowest span value for a single population of PS beads and with it the highest accuracy in characterization of the particle size distribution. All techniques showed similar particle size distribution percentile values, indicating similar accuracy in sizing of PS beads in the presented setting. Percentiles of obtained distributions are not presented for DLS as it is not recommended calculating these value because of the inherent errors present in the deconvolution of the correlation function used for particle measurements [34].

*Table 2. Descriptors of particle size distributions obtained from measuring single populations of PS203nm and PS799nm beads with DLS, NTA, RMM and MRPS. Values are presented as mean values of replicate measurements and errors are standard deviations of the triplicate measurements. Span represents width of the size distribution ((D$_{90}$-D$_{10}$)/D$_{50}$). *Parameters of main peak reported*

Technique	Bead diameter size (nm)	Mean diameter (nm)	Peak max (nm)	D$_{10}$ (nm)	D$_{50}$ (nm)	D$_{90}$ (nm)	Span
DLS*		234 ± 5	220 ± 0	-	-	-	-
NTA	203	193 ± 1	198 ± 2	166 ± 1	194 ± 1	213 ± 3	0.25 ± 0.06
MRPS		187 ± 7	178 ± 6	162 ± 2	182 ± 1	222 ± 2	0.33 ± 0.01
DLS*		879 ± 5	825 ± 0	-	-	-	-
RMM	799	805 ± 1	792 ± 4	747 ± 4	780 ± 1	822 ± 2	0.10 ± 0.01
MRPS		799 ± 15	758 ± 3	737 ± 12	792 ± 12	886 ± 10	0.19 ± 0.01

PS495nm beads were measured with the three techniques within the estimated concentration range from $1*10^6$ p/ml up to $1*10^{10}$ p/ml (Figure 3 A). All techniques showed strong linearity (>0.98) for measured bead concentrations within their working counting range.

For MRPS a concentration range of approximately $5*10^7-1*10^{10}$ p/ml could be covered with cartridge TS-900 and of $5*10^6-5*10^9$ p/ml with cartridge TS-2000. Consequently, MRPS was the only technique able to cover the entire concentration spectrum, showing a superior dynamic range compared to RMM and NTA. Although it was possible to carry out measurements at lower tested concentrations, the required number of measured particles stated in Materials and Methods section could not be reached within a practical timeframe (Figure 3 A, empty symbols).
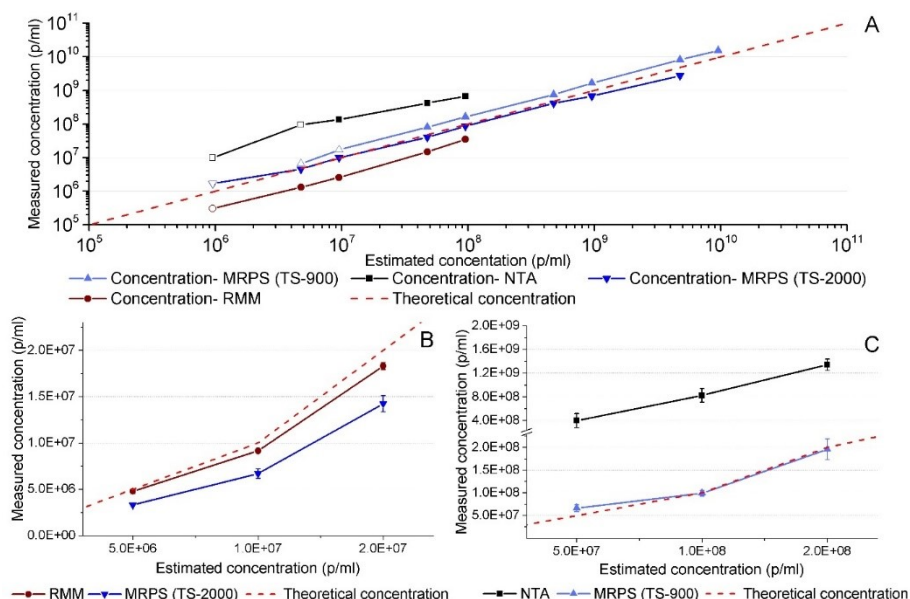

Figure 3: (A) Relation between theoretically estimated and measured concentration of PS495nm obtained by NTA, RMM and MRPS. Empty symbols represent measured samples with a particle concentration below the recommended concentration range for the given technique

Because of the limitations of RMM and NTA to detect PS495nm beads (see discussion section), we further investigated PS799nm and PS203nm beads to compare the relative accuracy and precision in quantification of nm-sized particles between MRPS, NTA and RMM. The PS beads were analyzed at three dilutions. For PS799nm, RMM reported higher measured particle concentrations compared to MRPS by 50% for the two lowest and by 25% for the one highest estimated concentrations (Figure 3 B). NTA determined a much higher particle concentration of PS203nm for all three dilutions compared to MRPS and showed

particle concentrations up to 8 fold higher compared to the estimated concentrations calculated based on manufacturer specifications (Figure 3 C).

The technique with the highest repeatability in determining particle concentration was RMM, which showed an average deviation of 3±2% for replicate measurements among the three concentrations. Precision in particle count for MRPS was dependent on the used cartridge and an average 5±3% and 10±3% deviation was found for TS-2000 and TS-900, respectively. NTA was the technique with the lowest precision in particle counting for which the deviation varied from 8% to 30% for the highest and lowest estimated PS bead concentration, respectively.

Size resolution of MRPS in comparison with DLS, NTA and RMM

In order to compare the size resolution and the ability to discriminate multimodal particle size distributions, PS297nm, PS495nm and PS799nm beads were analyzed individually and as mixtures (Figure 4). Gaussian curves were plotted for each distribution and the peak max, peak start and peak end was obtained. In addition, full width at half maximum (FWHM), which refers to the width of the peak at 50% of the peak height, was considered (Supplementary table S1). Furthermore, the impact of the polydispersity on the measured size distribution was investigated. The particle size distributions for the single particle counting techniques (NTA, RMM and MRPS) are presented in 10 nm bins, whereas DLS results are presented as a series of logarithmically spaced size bin values derived by the used software.
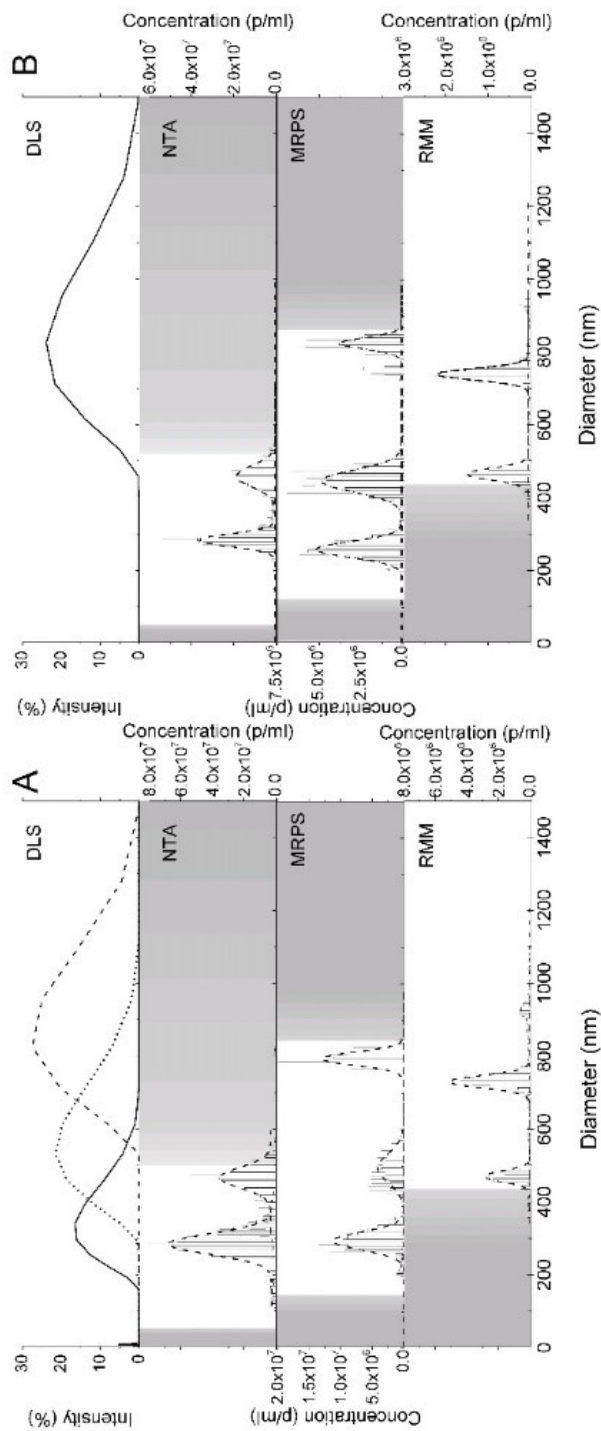
Figure 4: Particle size distributions of PS297nm, PS495nm and PS799nm beads (particle number ratio of 2:1:1) measured individually (A) and as mixture (B) with DLS, NTA, MRPS and RMM. Beads were dispersed in PBS (pH 7.4) + 0.1% w/v polysorbate 20 (RMM samples were free from polysorbate 20). Grey areas indicate particle sizes out of the approximate optimum working size range (white areas) for each technique, taking into account factors influencing the measurement, such as physical properties of particles (density, RI) and diluent (density, RI and conductivity).

Figure 4 A presents the particle size distributions of triplicate measurements of three monomodal bead populations (beads measured individually) performed by DLS, NTA, RMM and MRPS. For the characterization of nanometer-sized PS beads, DLS and MRPS proved to be superior to RMM or NTA with respect to the covered sizing range. Although DLS could cover the full size range presented in Figure 4 A, the technique showed the broadest peaks for monodisperse beads with FWHM values 5- to 15-fold greater compared to MRPS. It must be noted that DLS does not count individual particles but provides an intensity-weighted distribution of the overall population, which is naturally weighted according to the light scattering intensity of each particle fraction. Therefore, the obtained size distributions obtained with DLS will vary significantly to the other single particle analysis techniques and a direct comparison should not be performed. For NTA, RMM and MRPS the determined mean size diameter and FWHM values correlated well. Of note, RMM showed the highest precision in determination of particle size distribution.

Figure 4 B presents particle size distribution of multimodal PS bead suspensions (beads analyzed as mixture). Measurements with DLS showed only one single peak with a Z-average diameter of 785 nm. So, resolving different size populations at equal molar ratio was not possible, as shown before[35], and the strong bias towards larger particles in the intensity-weighted distribution provided by DLS displays the technique's inaccuracy in characterization of polydisperse samples. For the remaining techniques, the difference in mean size between each PS bead population was enough to resolve the different bead sizes present in the mixture. For NTA and RMM mean size diameter and peak max for each population group agreed well between both the measurements of individual and mixed beads with values falling within 5% of each other. For MRPS measurements of multimodal populations the determined mean size diameter of PS799nm beads was used to calibrate the cartridge. The variation in mean size diameter of PS297nm and PS495nm between monomodal and multimodal populations was 7% and 14%, respectively.

For quantitative determination of each technique's size resolution we used equation 1, which is commonly applied in chromatography to determine the degree of separation of

two solutes[36] and was used in a recent study on validation of the nanoparticle tracking analysis method[24]:

$$Rs = \frac{tR2 - tR1}{\frac{W1 + W2}{2}} \qquad (1)$$

Where, tR1 and tR2 are local maxima of peak 1 and peak 2, and W1 and W2 are peak width at baseline of these peaks. MRPS showed the highest R_s values compared to NTA and RMM, indicating high resolution capabilities in characterization of polydisperse samples.

Applications of MRPS for analysis of pharmaceutically relevant particulate formulations in comparison to RMM, DLS and NTA

Protein aggregates

The stressed BSA formulation was diluted by a factor of 25-, 50-, 100-, 250- and 500-fold in PBS and the dilutions were studied with DLS, NTA, RMM and MRPS within the suitable working range with respect to particle concentration for each technique (Figure 5). At each dilution level DLS showed multiple peaks, including a peak at ca. 10 nm deriving from BSA monomer and smaller aggregates. Subpopulations of particles above 20 nm were not resolved and the PDI value was above 0.9.
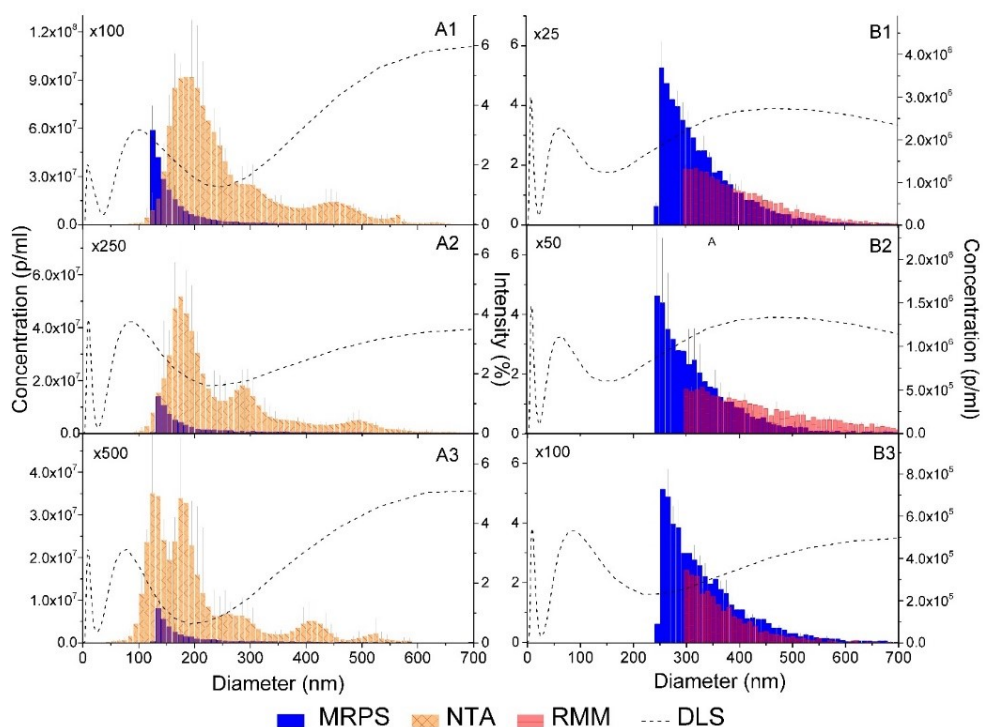
Figure 5: Particle size distribution of stressed BSA. A1-A3 show PSD determined with DLS, MRPS (TS-900) and NTA at 100-, 250- and 500-fold dilutions. B1-B3 show PSD determined with DLS, MRPS (TS-2000) and RMM at 25-, 50- and 100-fold dilutions. Middle Y-axes relate to determined intensity with DLS, whereas Y-axes on the left and right side represent the measured concentration for each bin size and their scale is adjusted to each graph. Error bars represent the standard deviation of triplicate measurements.

Figure 5 A1-A3 presents the particle size distributions of stressed BSA samples at 100-, 250- and 500-fold dilution, each measured with DLS, MRPS and NTA. The shape of the distribution determined with NTA shifted towards smaller sized particles for each subsequent dilution, whereas MRPS produced a consistent asymmetrical particle size distribution with a cut-off at a fixed lower limit of size detection. MRPS and RMM showed highly similar particle size distributions above 300 nm for protein aggregates at all three different dilutions (Figure 5 B1-B3).

The decrease in sensitivity of NTA for smaller particles within samples that also contain a higher number of larger particles, led to an underestimation in the concentration of particles below 200 nm. Nonetheless, compared to MRPS, NTA reported an approximately 10-fold higher determined particle concentration within the same measured size range for

each dilution. MRPS measured higher concentrations of particles above 300 nm compared to RMM, however the difference was below 18%.

Liposomes

Measurement of liposomes diluted 5000-fold in PBS was performed by using DLS, NTA and MRPS (Figure 6 A). DLS showed a Z-average diameter of 165 nm with a PDI of 0.09, indicating a homogenous particle size distribution. NTA showed a similar mean size diameter (159 nm) as DLS, with a relatively low average polydispersity of the size distribution (span-0.69) for each replicate. The mean size diameter determined with MRPS was 97 nm, which is significantly lower compared to the values obtained with the two light scattering-based techniques. Furthermore, MRPS produced a wider size distribution (span-1.23), suggesting a higher sensitivity towards the smallest and largest particles within the population.
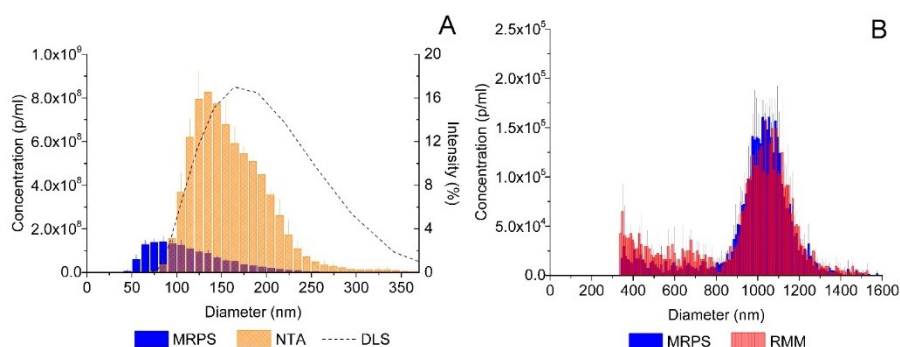

Figure 6: A) Particle size distribution of liposomes from NTA, DLS and MRPS (TS-400). For MRPS and NTA the determined particle concentration is reported on the left y-axis and the measured intensity with DLS is reported on the right y-axis. The diameter is shown in a logarithmic scale (x-axis). B) Particle size distribution of Lactobacilli determined by MRPS (TS-2000) and RMM. Error bars represent the standard deviation of the triplicate measurements.

Quantification of the number of liposomes was carried out with NTA and MRPS. The reported mean particle concentration with NTA was 5.5-fold greater when compared to MRPS, which confirms the data obtained from measurement of PS beads (Table 2 and Figure 3).

Lactobacilli

A commercially available product, containing a mixture of *Lactobacilli helveticus* and *Lactobacilli rhamnosus*, was used to examine the suitability of MRPS for counting and sizing microorganisms, and the performance of MRPS was compared to that of RMM (Figure 6 B). The mean size for the bacteria population was 1037 nm according to MRPS, which correlates well with the mean diameter of 1075 nm obtained with RMM.

Both techniques showed a similar concentration of *Lactobacilli*. The particle concentration within the size range 800-1600 nm, the expected size of the bacteria, was $3.52*10^6$ and $3.48*10^6$ p/ml for MRPS and RMM, respectively. Particles detected below ca. 800 nm are most likely cell debris or particulate matter originating from the stock material and were not included in the calculation.

Discussion

We evaluated the MRPS technique for particle characterization to provide insights into its limitations and advantages. The electrical conductivity of the analyzed sample showed to be one of the most important factors for correct analysis with MRPS. An underestimation of the particle diameter and an overestimation of particle counts at low ionic strength (below 3 mS/cm) of the analyte suspension were observed. Lower reported diameter sizes for PS beads in samples with low electrical conductivity relate to the relatively lower induced ΔR at the nanoconstriction upon particle passage at the orifice. This translates to a weaker output signal due to the decreased double-layer capacitance of the sensing electrode[37]. In addition, the thermal noise is increased at low ionic strength due to the reduced measurement bandwidth, leading to a higher baseline noise and increased number of false-positives (Supplementary figure S1) as well as a loss of particle detection at the lower end of the sizing range (Figure 2 A and 2 B). It must be noted that the conductivity threshold of 3 mS/cm applies solely to the TS-2000 cartridge and will increase in smaller cartridges which are equipped with a nanoconstriction of smaller orifice dimensions.

The apparent particle concentration increased in samples with a conductivity below 3 mS/cm. MRPS determines particle concentration based on the mean transit time of single particle passages via a high current density surrounding the nanoconstriction. This high current density is significantly reduced at a low concentration of ionic species, and therefore the magnitude of this electric field is reduced for a prolonged time and a higher transit time is detected by the software (Figure 2 C).

The cartridges are fabricated by using a micro-molding technique, where each batch is produced with a single mold with defined microfluidic channels. For accurate size determination it is recommended by the manufacture to spike in a reference standard (e.g., NIST PS beads) into the sample for a required size calibration. However, biological material, such as proteins, tend to irreversibly adsorb to PS beads, which may alter the size distribution of the PS particles as well as that of the analyte[38]. Moreover, the bead size may overlap with the size of particles in the sample. Because of the high intra-cartridge sizing precision shown within our study (Table 1), the size calibration measurement of each cartridge was performed after the sample measurement.

Furthermore, the accuracy and precision of the four particle characterization techniques was evaluated using PS203nm and PS799nm. The mean diameter size values obtained with NTA, RMM and MRPS are slightly lower compared to DLS and in better agreement to the reference value. This trend was expected, as the dispersed particles scatter incident light proportional to at least the 2nd power of their radii (depending on the particle size, wavelength of the used laser and type of scattering) leading to a bias towards larger particles size in DLS[39]. A similar trend was observed by other authors who performed sizing comparisons between DLS and NTA[22] or DLS and tunable resistive pulse sensing technique[40]. Furthermore, for both bead populations, MRPS, NTA and RMM showed a highly similar span values, indicating a similar accuracy in determination of the size distribution for monodisperse populations. The variation coefficient of the mean size determined with MRPS for PS beads was ca. 3-5%, which is superior to the repeability of NTA measurements stated in the literature (6.3% and 10% with software version 3.0 and 2.3, respectively)[24].

However, values above 3% are inferior to that of RMM (0.3%) and DLS (1.1%)[18], and to the results presented in Table 2.

DLS does not quantify particles, but is a qualitative technique for assessing particle size distributions with a high sensitivity, or bias, to larger aggregates/particles within an analyzed sample. Therefore, DLS was not considered for the comparison of the techniques with respect to particle quantification. The particle concentration determined by MRSP, NTA and RMM varied for each sample to a significant degree. Such deviations in determined particle concentrations from different methods have been previously reported and a number of factors could contribute to these[26,41]. Firstly, in all current techniques for submicron particle measurements, a notably small sample volume is analyzed and therefore the extrapolation factor of particle counts to particles/mL is relatively high. For example, in our setup, NTA analyzes up to 0.08 nL per replicate – generating an extrapolation factor of about $1*10^9$. The analyzed volume with MRPS is cartridge dependent. The TS-900 cartridge samples approximately 10 nL per replicate, yielding an extrapolation factor of about $1*10^5$. With the TS-2000 cartridge and also with RMM, 150 nL were analyzed, resulting in an extrapolation of particle count of approximately $1.5*10^4$. For comparison, methods used for characterization of micron sized particles, e.g., flow imaging microscopy, measure from 0.15 up to 0.8 mL of sample and particle counts are corrected to particles/mL by a factor of 6.5 - 1.25.

Secondly, an additional source of discrepancies in particle count between each technique could be the different measuring principle used to determine the absolute particle concentration. NTA takes the average count of particles per frame and then divides it by the interrogated volume determined by the cell dimensions. RMM and MRPS measure the particle concentration based on the single transit time of a particle through a microfluidic channel and a high current density, respectively. The different algorithms and models used in each method can introduce errors that may lead to imprecision in the obtained particle concentrations.

For the evaluation of size resolution, a mixture of three differently sized PS beads at a number ratio of 2:1:1 was considered as a suitable polydisperse model sample with no

overlap between particle size distributions of the three sets. The difference in mean size diameter between the PS297nm and PS799nm is above 2.5-fold, thus allowing to compare how well each instrument will be able to handle samples consisting of a broad range of particle sizes. Hence, for techniques with high resolution, the distinction of each population should be evident. In this study, we did not study other ratios of PS beads or the impact of concentration of distinct bead populations on the overall particle size distribution. Apart from DLS, all evaluated techniques showed good separation of peaks, with MRPS having the highest R_s value (Supplementary table S1). The incapability of resolving PS bead populations with DLS was expected, as discussed above. In the literature, NTA has been used to characterize PS particles from 30 nm up to 1000 nm in diameter[22,25,42]. However, the short wavelength laser used in our study limited the technique´s measurement capability of PS799nm due to the multiple scattering points present on a single particle, resulting in an interference that impedes correct particle tracking. Consequently, samples containing large particles may require additional sample preparation, e.g., filtration or centrifugation, prior to measurement with NTA for reliable characterization of the particle size distribution in the nanometer size range, as shown before for polydisperse protein aggregates[25]. RMM detects particles entering a microfluidic channel where they alter the resonance frequency of the suspended resonating cantilever[20]. The low density of PS beads (1.05 g/cm^3) suspended in PBS affects the lower limit of size detection and increases it automatically to 460 nm. This shows a critical limitation of RMM for the characterization of heterogeneous samples with particulate matter of low or unknown density where a significant error in the observed particle size distribution and particle concentration may be introduced.

Artificially stressed BSA samples were submitted to dilution and the proteinaceous particles were characterized by the four evaluated techniques. As different dilution factors may alter the protein particle concentration and/or size distribution[25], in our study comparative characterization was performed by measuring samples submitted to identical dilutions. MRPS showed to be capable of analyzing polydisperse proteinaceous samples on particle-by-particle basis to which sample dilution had not effect on the determined particle size distributions, as opposed to NTA or DLS. The bell shape distribution towards particles of larger sizes (clearly visible in Figure 5 A and 5 B) for protein aggregates seen with NTA has

been observed in the past by other authors[22,25,43]. Factors contributing to an inaccurate determination of particle size distribution by NTA for polydisperse samples include: 1) the relatively low particle counts obtained from a single measurement, as well as 2) the loss in sensitivity for smaller, weakly scattering particles, therefore showing bias towards a limited particle population. The derived Z-average diameter from DLS is an intensity-based overall average size based on a specific fit to the raw correlation function data. Therefore, the obtained data did not provide accurate information on particle populations within the sample, as this technique is not suitable for such polydisperse samples[18]. RMM and MRPS presented highly similar results for the proteinaceous samples with respect to particle size distribution and particle concentration.

For liposomes, DLS and NTA determined a higher mean size diameter of the population compared to MRPS, due to the above discussed bias of these techniques. Similar to protein aggregates, the difference in refractive index between buffer and liposomes is relatively small, resulting in a low light scattering intensity. Thus, the smallest particles within the population will not be detected with the two light scattering-based techniques and the reported distribution will be shifted to higher particle sizes. Additionally, the loss of sensitivity with NTA towards the smallest and largest particles within a polydisperse sample is indicated by the 2-fold smaller span value for liposome samples compared to MRPS (Supplementary table S2). Furthermore, the liposome concentration determined by NTA was significantly higher as compared to MRPS, which is in agreement with the results for PS beads (Figure 3). Previously reported comparative analysis between NTA and the resistive pulse sensing (RPS) technique, also showed an approximate 10-fold overestimation in concentration by NTA and the heavy influence of the operator settings on the quantitative assessment [44].

Characterization of bacterial cells using RMM and RPS was previously reported in the literature [33,45,46]. The two instruments determine the mean particle diameter via two distinct measuring principles using particle mass or volume, respectively. The obtained mean diameter values with RMM and MRPS vary from the cell dimensions of rod-shaped *Lactobacilli* stated in literature determined by using electron microscopy (*L. helveticus* – 6.0

x 0.7-0.9 μm and *L. rhamnosus* 2.0-4.0 x 0.8-1.0 μm)[47]. The measured diameters acquired with both used techniques refer to the volume-equivalent spherical diameter, which is characterized by:

$$d_V = \left(\frac{6}{\pi} V\right)^{\frac{1}{3}}$$

$$(2)$$

Where d_v is the diameter of a sphere with the same volume (V) as the particle. Using equation 2 and the reference bacteria dimensions to calculate d_v, we would expect the volumetric mean diameter to be in the range between 1.2 and 1.9 μm. Therefore, both MRPS and RMM may underestimate the mean size of elongated particles. These results align with the work carried out by Cavicchi et al., who showed a significant underestimation of d_V with the electrical sensing zone instrument for rod-shaped micrometer-sized particles[48]. The shape of particles would also have an impact on the reported mean diameter with DLS or NTA. Further investigation of the influence of particle shape and morphology on reported mean particle size and concentration with nanoparticle characterization techniques is therefore recommended.

Each of the evaluated technique in this study operates on a distinct principle. The suitability of each technique depends on the intended application, i.e., type of sample, required read-out and purpose of the analysis. In Table 3 we compare the four techniques to assist the reader in selecting the most appropriate technique for a given experimental setup. For instance, for a rapid and qualitative determination of the presence of particles, DLS can be recommended. However, for quantitative characterization of particle size distribution and particle concentration, single particle counting techniques (NTA, RMM, MRPS) are preferred. The other main factors to consider are the physical properties of the analyzed particles (e.g., size, refractive index, density, shape) and sample (e.g., viscosity, conductivity, particle concentration). As an example, highly concentrated protein solutions come along with a high viscosity and a high refractive index. In this case, the performance of light scattering-based techniques, such as NTA and DLS, is compromised, and RMM and MRPS

may be superior. With respect to highly viscous samples, software operating DLS, NTA and RMM allows the user to input the analyzed sample's viscosity. So far, such an option does not exist for the software operating MRPS and therefore, calibration beads of known size and concentration must be spiked into the sample to perform the required calibration.

Table 3. Comparison of the four evaluated techniques.

	DLS	NTA	RMM	MRPS
Technique characteristics				
Size determination based on	Intensity fluctuations of scattered light from particles moving under Brownian motion	Tracking the position of individual light-scattering particles moving under Brownian motion	Frequency shift of resonating cantilever	Electrical resistance increase in orifice
Approximate size range based on the literature [17,21]	1 – 1000 nm	30 – 1000 nm	300 – 5000 nm	50 – 2000 nm
Reported diameter	Hydrodynamic	Hydrodynamic	Volumetric	Volumetric
Approximate particle concentration range (#/mL) based on the literature [17,21]	$1*10^8 – 1*10^{12}$	$1*10^7 – 1*10^9$	$3*10^5 – 3*10^7$	$5*10^6 – 1*10^{11}$
Quantification and extrapolation factor for particle concentration	Not quantitative	Quantitative $\sim10^8$	Quantitative $\sim10^4$	Quantitative $\sim10^4$ (TS-900) or $\sim10^5$ (TS-2000)
Accuracy in size distribution determination of polydisperse particles	Low	Medium	High	High
Size resolution	Low	Medium	High	High
Technique's operative considerations				
Required information for (data) analysis	Refractive index, viscosity and temperature	Viscosity and temperature	Particle density	Conductivity
Additional requirements	-	-	System is vulnerable for blockage	Addition of polysorbate may be required for measurement
Consumables	Disposable or reusable cuvettes/plates	None	Microfluidic sensor	Microfluidic cartridges
Calibration	Not applicable	Not applicable	Required per sensor	Required per cartridge
Large particulate impurities or contaminants	Have significant influence on results	Easily detected and have large influence on results	May block the system and difficult to remove; little to significant impact on results	Filtered out at cartridge entry, no impact on results

Conclusions

MRPS showed to be a useful orthogonal technique for particle sizing and counting alongside DLS, NTA and RMM, which are frequently used in the (bio-)pharmaceutical field.. For measurements with nCS1 the sample of interest must have electrical conductivity above ~3 mS/cm for proper sizing and counting. Sizing of PS standard beads with each of the four techniques showed comparable results. Particle concentrations obtained by MRPS and RMM were similar, whereas NTA showed 5- to 10-fold higher particle counts. Apart from DLS, all techniques were able to resolve different size populations in polydisperse samples. The applicability of MRPS was further illustrated by the successful characterization of relevant samples, including protein aggregates, liposomes and bacteria. In conclusion, we have shown that MRPS is a valuable technique for analyzing particles in the nanometer- and low micrometer-size range.

Acknowledgments

References:

1. Tyagi P, Subramony JA. Nanotherapeutics in oral and parenteral drug delivery: Key learnings and future outlooks as we think small. J Control Release 2018;272:159-168.

2. Singh SK, Afonina N, Awwad M, Bechtold-Peters K, Blue JT, Chou D, Cromwell M, Krause HJ, Mahler HC, Meyer BK, Narhi L, Nesta DP, Spitznagel T. An industry perspective on the monitoring of subvisible particles as a quality attribute for protein therapeutics. J Pharm Sci 2010;99(8):3302-3321.

3. Narhi LO, Corvari V, Ripple DC, Afonina N, Cecchini I, Defelippis MR, Garidel P, Herre A, Koulov AV, Lubiniecki T, Mahler HC, Mangiagalli P, Nesta D, Perez-Ramirez B, Polozova A, Rossi M, Schmidt R, Simler R, Singh S, Spitznagel TM, Weiskopf A, Wuchner K. Subvisible (2-100 mum) particle analysis during biotherapeutic drug product development: part 1, considerations and strategy. J Pharm Sci 2015;104(6):1899-1908.

4. Kijanka G, Bee JS, Bishop SM, Que I, Lowik C, Jiskoot W. Fate of multimeric oligomers, submicron, and micron size aggregates of monoclonal antibodies upon subcutaneous injection in mice. J Pharm Sci 2016;105(5):1693-1704.

5. Roberts CJ. Protein aggregation and its impact on product quality. Curr Opin Biotechnol 2014;30:211-217.

6. Moussa EM, Panchal JP, Moorthy BS, Blum JS, Joubert MK, Narhi LO, Topp EM. Immunogenicity of therapeutic protein aggregates. J Pharm Sci 2016;105(2):417-430.

7. Weinbuch D, Jiskoot W, Hawe A. Light obscuration measurements of highly viscous solutions: sample pressurization overcomes underestimation of subvisible particle counts. AAPS J. 2014;16(5):1128-1131.

8. USP<788>. Particulate matter in injections. United States Pharmacopoeia, Natl. Formul. 2006.

9. Zolls S, Tantipolphan R, Wiggenhorn M, Winter G, Jiskoot W, Friess W, Hawe A. Particles in therapeutic protein formulations, Part 1: overview of analytical methods. J Pharm Sci 2012;101(3):914-935.

10. U.S. Department of Health and Human Services FaDA, Center for Drug Evaluation and Research, Center for Biologics Evaluation and Research. In: Guidance for industry: immunogenicity assessment for therapeutic protein products; 2014. Available at: http://www.fda.gov/Drugs/GuidanceComplianceRegulatoryInformation/Guidances/default.htm. Accessed March 30, 2018.

11. Carpenter JF, Randolph TW, Jiskoot W, Crommelin DJ, Middaugh CR, Winter G, Fan YX, Kirshner S, Verthelyi D, Kozlowski S, Clouse KA, Swann PG, Rosenberg A, Cherney B. Overlooking subvisible particles in therapeutic protein products: gaps that may compromise product quality. J Pharm Sci 2009;98(4):1201-1205.

12. Zhang L, Shi S, Antochshuk V. Closing the gap: counting and sizing of particles across submicron range by flow cytometry in therapeutic protein products. J Pharm Sci 2017;106(11):3215-3221.

13. Chuang S-Y, Lin C-H, Huang T-H, Fang J-Y. Lipid-based nanoparticles as a potential delivery approach in the treatment of rheumatoid arthritis. J Nanomater 2018;8(1):42.

14. Desai N. Challenges in development of nanoparticle-based therapeutics. AAPS J. 2012;14(2):282-295.

15. Kim OY, Park HT, Dinh NTH, Choi SJ, Lee J, Kim JH, Lee S-W, Gho YS. Bacterial outer membrane vesicles suppress tumor by interferon-γ-mediated antitumor response. Nat Commun 2017;8(1):626.

16. van der Pol E, Coumans FA, Grootemaat AE, Gardiner C, Sargent IL, Harrison P, Sturk A, van Leeuwen TG, Nieuwland R. Particle size distribution of exosomes and microvesicles determined by transmission electron microscopy, flow cytometry, nanoparticle tracking analysis, and resistive pulse sensing. J Thromb Haemost. 2014;12(7):1182-92

17. Bhattacharjee S. DLS and zeta potential – What they are and what they are not? J Control Release 2016;235:337-351.

18. Panchal J, Kotarek J, Marszal E, Topp EM. Analyzing subvisible particles in protein drug products: a comparison of dynamic light scattering (DLS) and resonant mass measurement (RMM). AAPS J. 2014;16(3):440-451.

19. Hawe A, Romeijn S, Filipe V, Jiskoot W. Asymmetrical flow field-flow fractionation method for the analysis of submicron protein aggregates. J Pharm Sci 2012;101(11):4129-4139.

20. Burg TP, Godin M, Knudsen SM, Shen W, Carlson G, Foster JS, Babcock K, Manalis SR. Weighing of biomolecules, single cells and single nanoparticles in fluid. Nature 2007;446:1066.

21. Godin M, Bryan AK, Burg TP, Babcock K, Manalis SR. Measuring the mass, density, and size of particles and cells using a suspended microchannel resonator. Appl Phys Lett 2007;91(12):123121.

22. Filipe V, Hawe A, Jiskoot W. Critical evaluation of nanoparticle tracking analysis (NTA) by NanoSight for the measurement of nanoparticles and protein aggregates. Pharm. Res. 2010;27(5):796-810.

23. Zhao H, Diez M, Koulov A, Bozova M, Bluemel M, Forrer K. Characterization of aggregates and particles using emerging techniques In Hanns-Christian Mahler WJ, eds. *Analysis of Aggregates and Particles in Protein Pharmaceuticals*, ed., John Wiley & Sons, Inc.; 2012:133-167.

24. Kestens V, Bozatzidis V, De Temmerman P-J, Ramaye Y, Roebben G. Validation of a particle tracking analysis method for the size determination of nano- and microparticles. J Nanopart Res 2017;19(8):271.

25. Tian X, Nejadnik MR, Baunsgaard D, Henriksen A, Rischel C, Jiskoot W. A comprehensive evaluation of nanoparticle tracking analysis (NanoSight) for characterization of proteinaceous submicron particles. J Pharm Sci 2016;105(11):3366-3375.

26. Rios Quiroz A, Lamerz J, Da Cunha T, Boillon A, Adler M, Finkler C, Huwyler J, Schmidt R, Mahler HC, Koulov AV. Factors Governing the Precision of Subvisible Particle Measurement Methods - A

Case Study with a Low-Concentration Therapeutic Protein Product in a Prefilled Syringe. Pharm Res 2016;33(2):450-461.

27. Filipe V, Hawe A, Carpenter JF, Jiskoot W. Analytical approaches to assess the degradation of therapeutic proteins. Trends Analyt Chem 2013;49:118-125.

28. Song Y, Zhang J, Li D. Microfluidic and nanofluidic resistive pulse sensing: A review. Micromachines 2017;8(7):204.

29. Maxwell JC. *A treatise on electricity and magnetism, 3rd ed*., New York: Dover Publications, Inc.; 1954:419-425.

30. Fraikin J-L, Teesalu T, McKenney CM, Ruoslahti E, Cleland AN. A high-throughput label-free nanoparticle analyser. Nat Nanotechnol 2011;6:308.

31. Barnett GV, Perhacs JM, Das TK, Kar SR. Submicron Protein Particle Characterization using Resistive Pulse Sensing and Conventional Light Scattering Based Approaches. Pharm Res 2018;35(3):58.

32. Varypataki EM, van der Maaden K, Bouwstra J, Ossendorp F, Jiskoot W. Cationic Liposomes Loaded with a Synthetic Long Peptide and Poly(I:C): a Defined Adjuvanted Vaccine for Induction of Antigen-Specific T Cell Cytotoxicity. AAPS J. 2015;17(1):216-226.

33. Lewis CL, Craig CC, Senecal AG. Mass and density measurements of live and dead Gram-negative and Gram-positive bacterial populations. Appl Environ Microbiol 2014;80(12):3622-3631.

34. Malvern Panalytical. 2016 D90, D50, D10, and span – for DLS? Available at: http://www.materials-talks.com/blog/2016/08/25/d90-d50-d10-and-span-for-dls/. Accessed March 23, 2018

35. Engelsman JD, Kebbel F, Garidel P. Laser light scattering-based techniques. In Mahler H-C, Jiskoot W, eds. *Analysis of Aggregates and Particles in Protien Pharmaceuticals, ed.,* New Jersey, USA: John Wiley & Sons.; 2012:43-49.

36. Foley JP. Resolution equations for column chromatography. Analyst 2012;116(12):1275-1279.

37. Bard AJ, Faulkner LR. *Electrochemical methods: Fundamentals and applications. ed*., Wiley.; 2000

38. Nejadnik MR, Jiskoot W 2015. Measurement of the average mass of proteins adsorbed to a nanoparticle by using a suspended microchannel resonator. J Pharm Sci 104(2):698-704.

39. Yguerabide J, Yguerabide EE. Light-scattering submicroscopic particles as highly fluorescent analogs and their use as tracer labels in clinical and biological applications: I. theory. Anal Biochem. 1998;262(2):137-156.

40. Pal AK, Aalaei I, Gadde S, Gaines P, Schmidt D, Demokritou P, Bello D. High resolution characterization of engineered nanomaterial dispersions in complex media using tunable resistive pulse sensing technology. ACS Nano 2014;8(9):9003-9015.

41. Anderson W, Kozak D, Coleman VA, Jamting AK, Trau M. A comparative study of submicron particle sizing platforms: accuracy, precision and resolution analysis of polydisperse particle size distributions. J Colloid Interface Sci 2013;405:322-330.

42. Kestens V, Bozatzidis V, De Temmerman P-J, Ramaye Y, Roebben G. Validation of a particle tracking analysis method for the size determination of nano- and microparticles. J. Nanoparticle Res 2017;19(8):271.

43. Vasudev R, Mathew S, Afonina N. Characterization of submicron (0.1-1 mum) particles in therapeutic proteins by nanoparticle tracking analysis. J Pharm Sci 2015;104(5):1622-1631.

44. Maas SLN, de Vrij J, van der Vlist EJ, Geragousian B, van Bloois L, Mastrobattista E, Schiffelers RM, Wauben MHM, Broekman MLD, Nolte-'t Hoen ENM. Possibilities and limitations of current technologies for quantification of biological extracellular vesicles and synthetic mimics. J Control Release 2015;200:87-96.

45. Yu ACS, Loo JFC, Yu S, Kong SK, Chan T-F. Monitoring bacterial growth using tunable resistive pulse sensing with a pore-based technique. Appl Microbiol Biotechnol 2014;98(2):855-862.

46. Cermak N, Becker JW, Knudsen SM, Chisholm SW, Manalis SR, Polz MF. Direct single-cell biomass estimates for marine bacteria via Archimedes' principle. ISME J 2016;11:825.

47. Schleifer K-H. Phylum XIII. Firmicutes Gibbons and Murray 1978, 5 (Firmacutes [sic] Gibbons and Murray 1978, 5). In De Vos P, Garrity GM, Jones D, Krieg NR, Ludwig W, Rainey FA, Schleifer K-H, Whitman WB, editors. *Bergey's Manual® of Systematic Bacteriology: Volume Three The Firmicutes, ed.,* New York, NY: Springer New York.; 2009:19-1317.

48. Cavicchi RE, Carrier MJ, Cohen JB, Boger S, Montgomery CB, Hu Z, Ripple DC. Particle shape effects on subvisible particle sizing measurements. J Pharm Sci 2017;104(3):971-987.

Supplementary materials
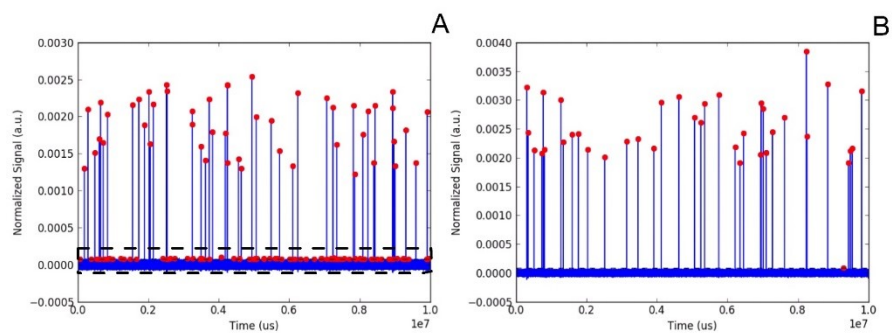
Supplementary figure S1: Output signal versus time for PS1030nm suspended in Na_2HPO_4 solution with low Na_2HPO_4 concentration (5mM) (A) and high Na_2HPO_4 concentration (150mM) (B). Events marked with red circle represent particle detection. Selected events in the dashed black rectangle represent detected false-positive events.

Supplementary table S1: Characterization of mono- and multimodal dispersions of beads using DLS, NTA, RMM and MRPS

Technique	PS beads	Mean diameter (nm)	Peak start (nm)	Peak max (nm)	Peak end (nm)	FWHM (nm)	R_s
DLS	Mono PS297nm	337 ± 5	181 ± 15	342 ± 0	647 ± 56	249 ± 21	
	Mono PS495nm	561 ± 3	326 ± 27	531 ± 0	1006 ± 88	382 ± 37	-
	Mono PS799nm	879 ± 5	615 ± 0	825 ± 0	1281 ± 0	467 ± 7	
	Multi	833 ± 8	507 ± 41	825 ± 0	1348 ± 117	508 ± 38	
NTA	Mono PS297nm	289 ± 2	181 ± 66	288 ± 5	391 ± 37	70 ± 21	
	Multi PS297nm	282 ± 19	235 ± 17	285 ± 0	338 ± 25	45 ± 17	1.38
	Mono PS495nm	432 ± 5	301 ± 15	451 ± 23	561 ± 30	86 ± 39	
	Multi PS495nm	459 ± 19	391 ± 25	455 ± 0	535 ± 36	71 ± 18	
RMM	Mono PS495nm	511 ± 1	440 ± 0	480 ± 0	517 ± 3	35 ± 1	
	Multi PS495nm	502 ± 1	433 ± 5	470 ± 0	513 ± 6	39 ± 4	3.56
	Mono PS799nm	830 ± 6	720 ± 17	760 ± 0	810 ± 0	33 ± 4	
	Multi PS799nm	812 ± 2	727 ± 6	760 ± 0	810 ± 0	37 ± 6	
MRPS	Mono PS297nm	296 ± 15	258 ± 15	285 ± 17	355 ± 10	50 ± 8	
	Multi PS297nm	260 ± 11	261 ± 11	251 ± 6	311 ± 23	43 ± 8	2.41
	Mono PS495nm	499 ± 34	438 ± 30	498 ± 47	578 ± 37	77 ± 9	
	Multi PS495nm	466 ± 20	401 ± 15	428 ± 12	498 ± 20	59 ± 14	
	Mono PS799nm	799 ± 15	765 ± 20	792 ± 12	832 ± 15	37 ± 10	4.71
	Multi PS799nm	801 ± 43	772 ± 42	798 ± 38	832 ± 49	34 ± 5	

Supplementary table S2: Span of particle size distribution of PS beads and liposomes measured with MRPS and NTA. Mean values and standard deviations of triplicate measurements (n=3)

Technique	PS297nm beads	Liposomes
	Span	
MRPS	0.33 ± 0.01	1.12 ± 0.04
NTA	0.25 ± 0.06	0.67 ± 0.01